

*ARMY RESEARCH LABORATORY*



---

# X-ray Shielding Requirements for a Reltron

Christopher S. Kenyon

---

ARL-TR-2440

October 2001

Approved for public release; distribution unlimited.

The findings in this report are not to be construed as an official Department of the Army position unless so designated by other authorized documents.

Citation of manufacturer's or trade names does not constitute an official endorsement or approval of the use thereof.

Destroy this report when it is no longer needed. Do not return it to the originator.

# Army Research Laboratory

Adelphi, MD 20783-1197

---

ARL-TR-2440

October 2001

## X-ray Shielding Requirements for a Reltron

Christopher S. Kenyon

Sensors and Electron Devices Directorate

---

## Abstract

---

Radiological dose rates from X-rays produced by a reltron (relativistic electron tube) microwave tube are calculated via standard electron-photon Monte Carlo transport software from the Integrated TIGER\* Series developed by Sandia National Laboratories, Albuquerque, NM. Comparison of an extrapolation of this dose rate for several hypothetical thicknesses of lead shielding surrounding this reltron with the standard maximum worker-allowed radiation level predicts the thickness of lead shielding required in the design of the reltron. Using worst case modeling for the X-rays, the required amount of lead shielding is, roughly, 1 ton.

\*TIGER is not an acronym

---

## Contents

---

<b>1. Introduction</b>	<b>1</b>
<b>2. The Reltron</b>	<b>2</b>
2.1. Description .....	2
<b>3. X-ray Computations</b>	<b>6</b>
3.1. Integrated TIGER Series of Electron-Photon Monte Carlo Transport Codes .....	6
3.2. Monte Carlo Calculation .....	6
<b>4. Results and Conclusions</b>	<b>11</b>
<b>References</b>	<b>13</b>
<b>Appendix A. Sample CYLTRAN Input File</b>	<b>15</b>
<b>Distribution</b>	<b>17</b>
<b>Report Documentation Page</b>	<b>19</b>

## Figures

1. Schematic of reltron in a cross-sectional view .....	3
2. Schematic of beam dump section of reltron in side view .....	3
3. Reltron electron beam energy distribution measured by Bruce Miller of Titan, Inc .....	3
4. Trajectories of 30-keV electrons in reltron beam dump section as they strike the anode .....	4
5. Trajectories of 100-keV electrons traveling down the reltron dump chamber, calculated by the PIC code MAGIC .....	5
6. Reltron beam dump diagram overlaid by a diagram of the CYLTRAN input computer model that was used to calculate X-ray production .....	8
7. Cross-sectional view of reltron beam dump chamber overlaid by its CYLTRAN model, including water "detectors" for determining x-ray flux at those locations .....	9

**Figures (cont'd)**

8. Cross-sectional view of reltron beam dump chamber overlaid by its CYLTRAN model with nine water “detectors” for determining x-ray flux variation in the vertical direction parallel to the reltron axis .....	9
9. Spatial variation of dose rate or equivalent dose rate equivalent computed for detectors at a distance of 30 cm from reltron .....	10
10. Extrapolated fits of calculated dose rates or effective dose rate equivalent compared with safety standards .....	11

---

## 1. Introduction

---

A reltron (relativistic electron tube), or relativistic electron tube, is a device for generating pulsed, high-power microwaves. Applied electric fields in the tube first “bunch” and then accelerate electrons to relativistic speeds. The bunched pulses then become a powerful source of microwave energy. When these relativistic electrons strike the tube’s copper anode, they produce an enormous amount of X-ray energy by *bremsstrahlung* radiation of the decelerating electrons. The production of X-rays is high, not only because of the high electron energy but also because of the high electron currents in the tube. The X-rays emanate in all directions from the tube but emerge from both the cylindrical side and the anode end with the greatest intensity. If no shielding is present to absorb the X-rays, then a nearby user of the reltron could easily receive a lethal dose in less than a second.

Clearly, the operation of a reltron requires the presence of either an excellent shield or a combination of a shield and user distance from the device. This report presents estimates of the X-ray radiation intensity that emerges from several different thicknesses of lead shielding surrounding the reltron. From these results, the author estimates the thickness of lead shielding necessary to protect a nearby user to within standard radiation exposure limits.

---

## 2. The Reltron

---

### 2.1. Description

The four sections of the reltron shown in figure 1 are the cathode (which emits the electrons), the buncher chamber, the acceleration gap, and the anode. The reltron was designed and built by Titan, Inc. The buncher applies alternating electric fields with or against the beam flow to bunch or create regular pulses of electrons. Next, the pulsed beam passes through a gap, accelerating it to nearly the speed of light. In our case, 450 kV are applied across the gap. Since the beam should now have many more electrons with approximately the same speed (close to light), the beam pulses are more coherent and more efficiently radiate high power radio frequency (RF) energy from the wave guide in the next section. On the right of figure 1 is the anode where the beam terminates and allows completion of the electrical circuit for the electrons to return.

The anode is housed in a section called the “beam dump chamber.” In practice, the reltron is oriented 90° to the left so that the anode or beam dump section is at the top, and future references will refer to it with this orientation assumed. The beam dump chamber was built by Communication Power Industries, Inc. The anode is copper and is surrounded by a water-cooling system shown in figure 2. This construction dissipates the heat produced by collision of the beam with the anode. A water tank surrounds the top and circulates water in a tube between a copper jacket and the anode.

The beam current is 220 A over a pulse width of 2  $\mu$ s. During operation, the pulse rate is 300 Hz within a 90-s “on” period. The duty cycle is 90 s on and 15 min off. The current density within the beam is about  $3.6 \times 10^4$  A/m<sup>2</sup>.

Figure 2 shows paths of electrons diverging under the influence of the local electric fields as they approach the anode. The paths shown are not the results of calculations but are merely illustrative. Electrons striking the anode have a distribution in energy ranging from about 0.02 to 1.14 MeV as measured\* by Bruce Miller at Titan, Inc., and shown in figure 3. The distribution peaks near 200 keV. The beam has a diameter of about 2.6 in. In the operation of a reltron, the highest energy electrons have an enormous momentum and will go straight down the axis of the beam dump chamber. Lower energy electrons may bow outward toward the anode walls more because the local electric fields will have a relatively larger impact on their velocities. Thus the incident energy distribution at the walls will be “cooler” toward the sides and “hotter” at incident radii shorter than 1.3 in. The cooler electrons will thus produce lower energy X-rays emerging more from the sides than those coming from the hotter electrons.

---

\*Personal Communication, Bruce Miller, Titan Laboratories, Inc.

Figure 1. Schematic of relatron in a cross-sectional view. (The beam dump section where the X-rays originate is on the right. In actual operation, the beam dump is at the top and X-rays emanate vertically from its top and radially outward from its sides. The intensity downward is far less than directions slightly upward from the horizontal.)

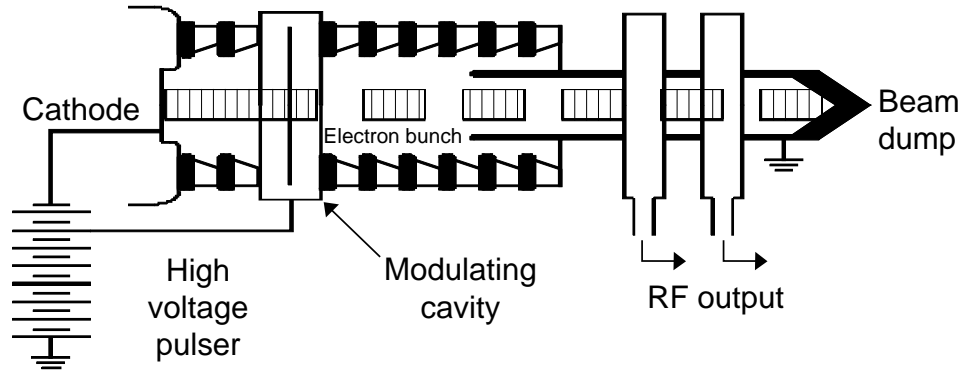


Figure 2. Schematic of beam dump section of relatron in side view. (The vertical line across the left side of the chamber represents the beam entry plane referred to in the text. The electrons travel down the axis toward the anode with a distribution of directions and speeds. They have, in general, a strong axial component which is complemented by a significant outward radial component developed by the local electric fields. The copper anode and its water-cooling system are designed to dissipate the thermal energy produced when the high energy electron current impacts it. The beam dump section is cylindrically symmetrical.)

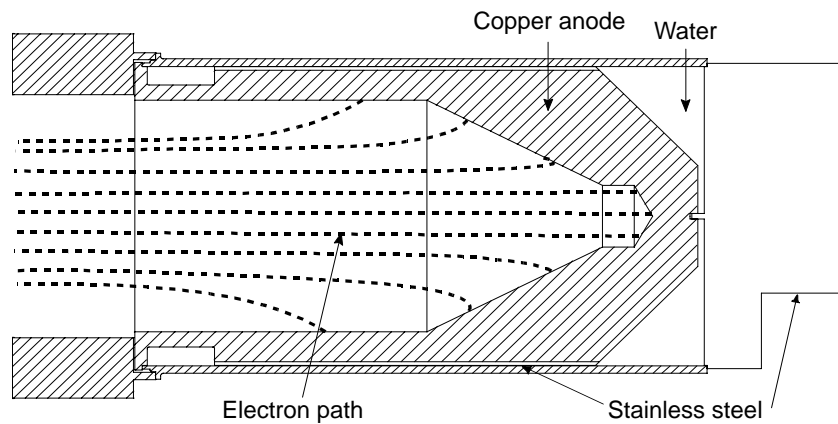
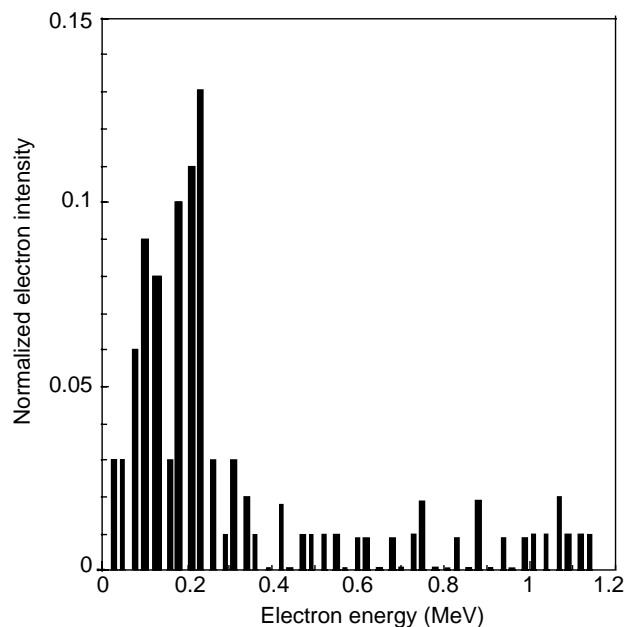


Figure 3. Relatron electron beam energy distribution measured by Bruce Miller of Titan, Inc.



To be more certain of the bounds on electron path divergence toward the reltron sides, electron paths were computed with a simplified model of the reltron. Version 4.0 of the Particle-in-Cell (PIC) code, "MAGIC," written by Mission Research Corporation [1], was run with electrons with energies within the energy range of electrons striking the anode. The calculations assumed beams of mono-energetic electrons initially traveling parallel to the axis toward the anode. Electron energy in MAGIC was specified by  $\gamma v$ , in which  $\gamma = 1/\sqrt{1 - v^2/c^2}$  and  $v$  and  $c$  are the electron velocity and the speed of light, respectively. Therefore, the low end of the spectrum had a  $\gamma v$  of about  $0.5 \times 10^8$  m/s and the high end was about  $9 \times 10^8$  m/s. Figures 4 and 5 show computed electron paths for energies of 0.03 MeV ( $\gamma v = 1 \times 10^8$  m/s) and 0.1 MeV ( $\gamma v = 2 \times 10^8$  m/s), respectively. In both cases, the beam divergence is weak and is weaker at higher energies.

Consequently, a model that assumes a beam electron energy distribution independent of direction and location of its incidence upon the anode walls will generate more energetic X-rays from the sides of the reltron than the actual distribution will. By using a uniform distribution, the model in these shielding calculations then predicted a worst case, or upper boundary, on the radiation. Specifically, this model assumed that the beam had a  $30^\circ$  spread from its axis with an origin at the entry plane shown in figure 2. A comparison of this spread with figures 4 and 5 shows that the model used for beam incidence in the ITS calculations has a broader spread than is likely to be the case as predicted by the MAGIC calculations. Therefore, the Integrated TIGER Series (ITS) calculations will clearly predict more X-rays emerging from the sides than is likely to be the case.

Figure 4. Trajectories of 30-keV electrons in reltron beam dump section as they strike the anode. (Trajectories were calculated by the computer program, MAGIC [1]. Weak radial divergence from the reltron axis at  $r = 0$  is evident.)

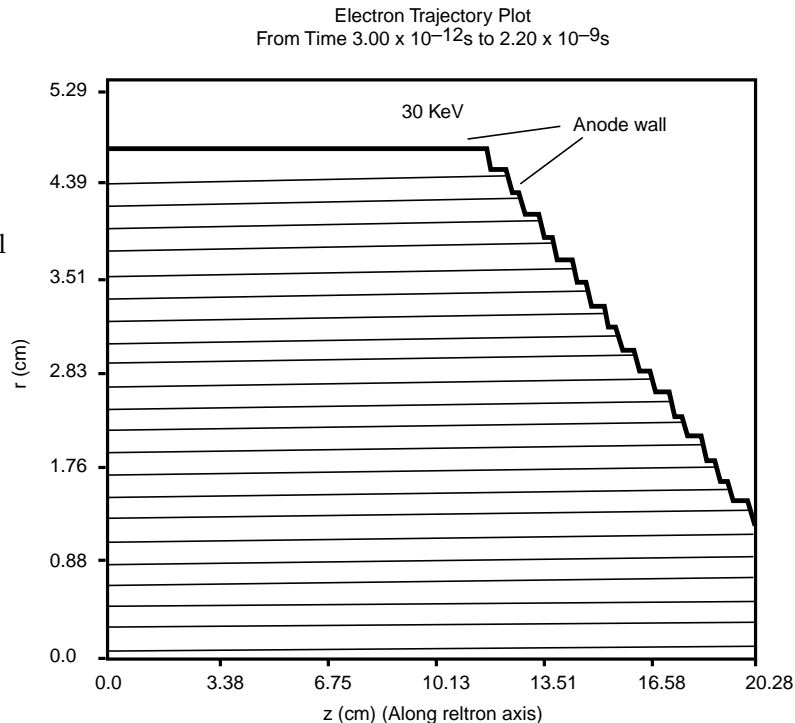
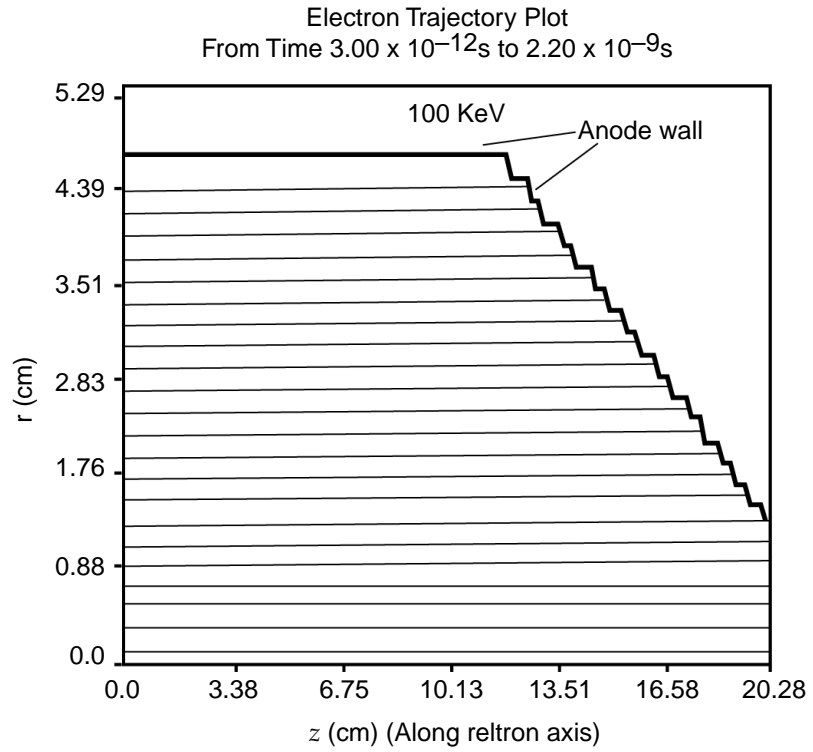


Figure 5. Trajectories of 100-keV electrons traveling down the reltron dump chamber, calculated by the PIC code MAGIC. (Little radial divergence from the axis at  $r = 0$  is seen for these higher energy electrons.)



---

## 3. X-ray Computations

---

### 3.1. Integrated TIGER Series of Electron-Photon Monte Carlo Transport Codes

The author calculated the X-ray radiation using the ITS computer codes. ITS computer codes are software programs written by Sandia National Laboratories, Albuquerque, NM [2] for a solution of linear, time-independent coupled electron-photon radiation transport problems. ITS consists of four parts: electron-photon cross-sectional data, a cross-sectional generation program, the Monte Carlo program, ITS, and the update emulator (UPEML).

The ITS source deck contains the FORTRAN source code for a variety of Monte Carlo codes that differ in ability to handle different material geometries, external electromagnetic fields, and cross-sectional data. UPEML extracts the particular desired source code from the ITS source deck, adjusts parts of the programs for use on different kinds of computers, and uniformly introduces other specific changes to an entire collection of ITS codes.

The basic procedure for use of the ITS codes first requires compilation of UPEML to create an executable code on the computer a person uses. Then, a user generates the FORTRAN source for both the cross-sectional generation program and the Monte Carlo program via UPEML. Execution of the cross-sectional program for the desired materials (e.g., copper, lead, water) and expected particle energy range creates cross-sectional data for use by the Monte Carlo program. The Monte Carlo program subsequently executes with input that specifies material geometries, particle source characteristics (e.g., electron directions and energies), and other parameters. Results of the calculations include energy and charge deposition in pre-specified zones and photon flux intensities and energies.

### 3.2 Monte Carlo Calculation

The ITS programs use Monte Carlo techniques to compute electron-photon transport through materials of various sizes and shapes. The Monte Carlo program starts by randomly selecting initial electrons (or photons) with energies and directions from distributions corresponding to the actual distributions to be modeled. When energetic electrons strike materials, they produce photons of various energies as well as secondary electrons of various energies. The photons produce or cause ejection of secondary electrons. The secondary electrons then produce photons and so forth. Each of these reactions consumes or divides the original particle energy so that all particle energies rapidly decline through the course of a history. A dominant mechanism of photon production is *bremsstrahlung* production of photons or X-rays, but photons are also produced in other ways, particularly when the electrons have lower energies. The ITS codes, by using known

probabilities or cross sections for photon and electron production from the collisions and the physics of particle trajectory mechanics, track and tabulate production and “death” of these particles through materials, starting with thousands or millions of sample electrons. The tracking of each original sample electron and all of its progeny represents one history. The history ends when the energy of the parent electron and that of every one of its progeny have dropped below a chosen low or “cutoff” energy or have exited the space given.

The ITS codes are one of three basic types: TIGER<sup>1</sup> for one-dimensional geometries, CYLTRAN for cylindrical geometries, and ACCEPT<sup>1</sup> for fully three-dimensional material geometries. For each of the codes, the transport is done in three-dimensions. However, selection of one of these three basic types limits the description of the shapes of the volumes through which the electron-photon transport is calculated. The reltron is basically cylindrical and the shielding for it would clearly have cylindrical symmetry. Consequently, a version of CYLTRAN would be an appropriate choice. CYLTRANP<sup>1</sup> uses a more comprehensive collection of collision or reaction types than CYLTRAN and should therefore give more accurate results. For this reason, the author used the cylindrical geometry ITS code, CYLTRANP, to calculate the X-ray radiation penetrating hypothetical cylindrical lead shields surrounding the reltron tube.

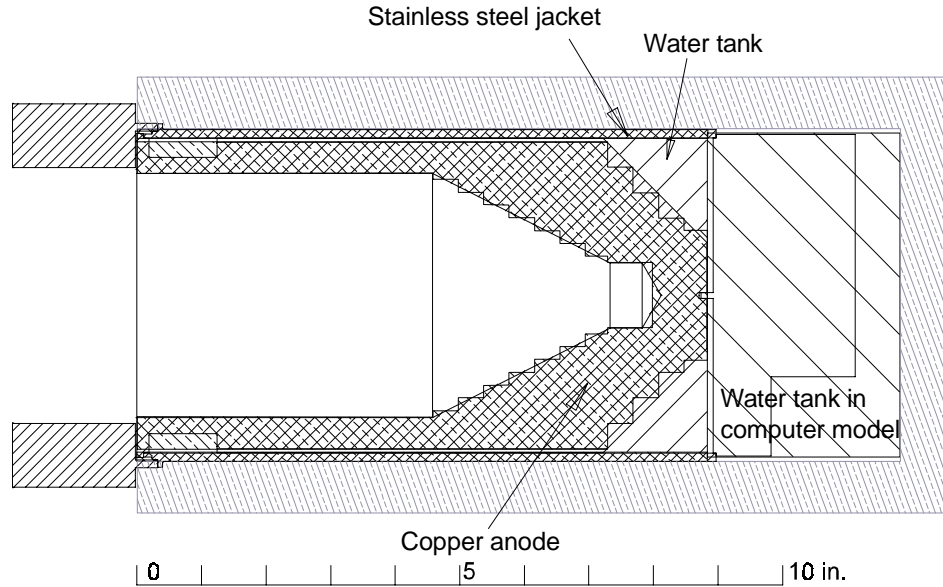
Several discrepancies between the actual beam dump chamber and its computer model introduced some error into the X-ray attenuation calculations. However, these are all small because the most important features in the model are (a) the thickness of the lead shield and (b) the thick copper anode. CYLTRANP models material volumes with collections of right circular cylinders or cylindrical “shells” that share a common axis. This restriction on volume descriptions required “stair-stepping” approximations of the copper anode, as shown in figure 6. Since the potential differences in photon transit lengths through the copper, which result from the steps compared to volumes without the steps, are small, this approximation should give reasonable results. The fact that attenuation of the X-rays in copper is only about 1/10 of that for lead should minimize the impact of this discrepancy. The actual beam dump chamber had a thin stainless steel jacket (see fig. 6) rather a copper one used in the model. However, the attenuation in steel and copper is very close, minimizing the consequential error this introduces into the calculation. The water tank used in the computer model is much larger than that in the beam dump chamber. However, because the attenuation of X-rays in water is roughly 1/30 of that for copper, the impact on the results should be small.

A “radiation absorbed dose” or rad is defined as 100 ergs of energy deposited into 1 gram of material by a radiation source such as X-rays or high energy particles. To determine the dose in rads by the CYLTRANP computation, water “detectors” were placed at sites closest to the reltron where a user might be located. Water was used because its radiation absorption

---

<sup>1</sup>Not an acronym.

Figure 6. Reltron beam dump diagram (see fig. 2) overlaid by a diagram of the CYLTRAN input computer model that was used to calculate X-ray production. (The CYLTRAN input model is uniquely depicted by hatching slanted to the left. The CYLTRAN X-ray detector volumes are not shown in this view. The CYLTRAN input model requires a composite of cylinders, each for a specific material. This requirement results in the stair-stepping approximation to the copper anode. Besides the stair-stepping discrepancy, the stepped right end of the copper anode model is a little short. A significant discrepancy is the difference between the actual water tank and the computer model for the water tank. The dump chamber assembly water tank consists of the triangular area rotated about the chamber axis, whereas the computer model used the large cylinder at the end.)



characteristics closely match those of a person. As in the case of shielding, the detectors are not real but are a convenient tool of the calculation. The detectors were placed 30 cm from the reltron axis, with positions at locations vertically displaced from a baseline across from the beam entry plane in figure 2 as shown in figures 7 and 8. Because of the limitations of volume descriptions in CYLTRANP, the detectors were cylindrical rings. Figure 7 shows, as an example, a side or cross-sectional view of the beam dump chamber, a lead shield around it, and two large cylindrical detectors centered on the beam axis.

The energy deposited into these detectors was computed by CYLTRANP. That energy divided by the mass of the detector is directly proportional the dose it received per beam electron. The larger the size of the detector, the more sensitive it is. However, ideally, the detector size should be smaller than the distance over which the radiation dose changes significantly. This restriction appears to be violated for the case of Detector 2 in figure 7, since the flux or dose from a point source falls as the inverse square of the distance. On the other hand, the attenuation of the X-rays by the water, even for the sizes of these detectors, is small.

To estimate spatial variation of dose, Detectors 1 and 2 shown in figure 7 were approximately replaced with nine thin detectors as shown in figure 8. Again, these are contiguous ring detectors centered about the reltron axis.

For humans, the dose in rads is within 1 or 2 percent of the effective dose equivalent in roentgen equivalent man (rem). Since this difference is far

Figure 7. Cross-sectional view of reltron beam dump chamber overlaid by its CYLTRAN model, including water "detectors" for determining x-ray flux at those locations. (The detectors are cylindrical rings with axes coinciding with the reltron beam axis. The beam axis is the line passing through the hollow point at the end of the beam dump chamber. Absorption of x-rays in water approximates absorption of x-rays in a human body very well. Below Detector 1 (i.e., to the left, here), the x-ray flux drops off rapidly. The 0 mark on the centimeter ruler also coincides with the beam entry plane of the beam dump chamber. The beam entry plane is perpendicular to the ruler. Both the large detectors shown here and smaller detectors referred to in figure 8 have inner radii of 30 cm. These detectors are 7 cm thick and 40 cm tall. Because of their volume being 7 times larger, they are 7 times as sensitive as the smaller detectors in figure 8.)

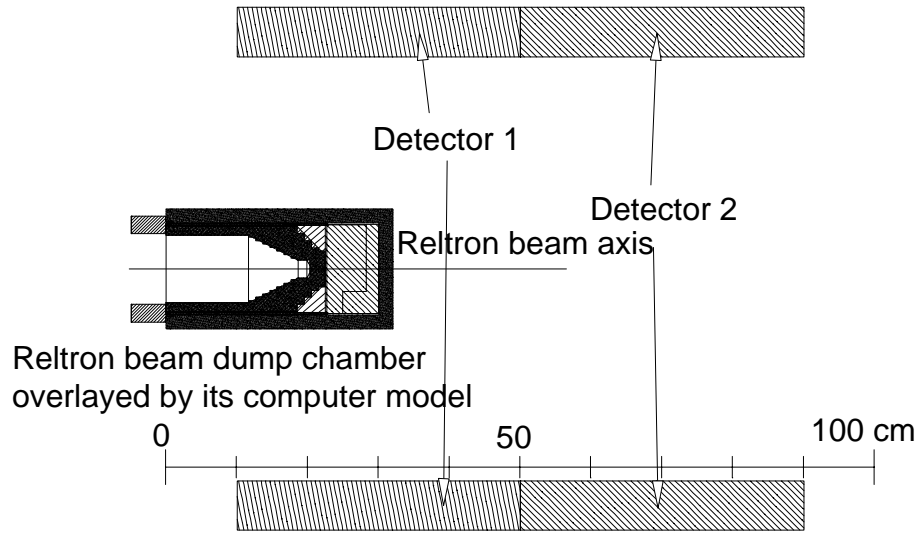
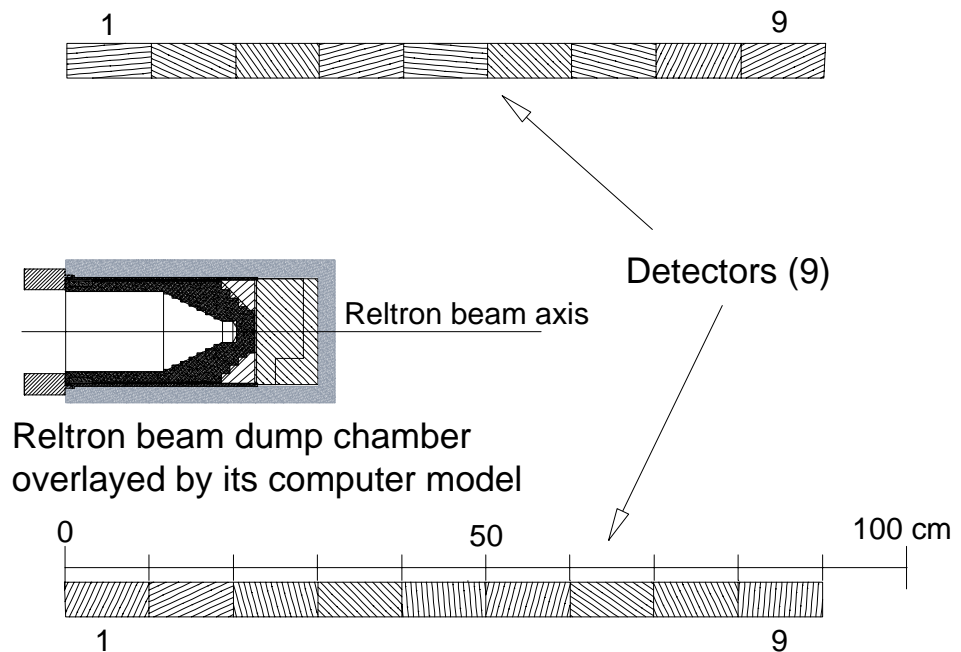


Figure 8. Cross-sectional view of reltron beam dump chamber overlaid by its CYLTRAN model with nine water "detectors" for determining x-ray flux variation in the vertical direction parallel to the reltron axis. (In this case, the nine detectors are nine contiguous cylindrical rings with axes coinciding with the reltron beam axis. The detector rings are 4 cm thick by 10 cm tall and their inner radii is 30 cm. These detectors were used to estimate the variation with vertical distance of the x-ray radiation escaping the shielded reltron. The first (1) and last (9) rings are explicitly labeled. Plots of the effective dose equivalent are shown in figure 9.)

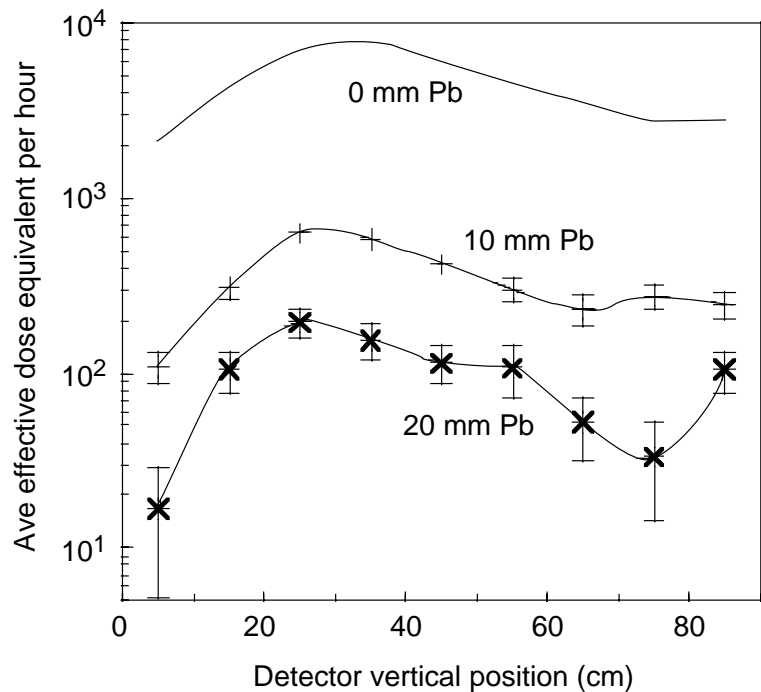


below the uncertainty in the final results, it is ignored in this report and for the purposes of this report, the effective dose equivalent and dose are the same.

The data of figure 9 show the spatial variation of dose or dose rate measured by these detectors at the closest distance users might be to the reltron. In particular, figure 9 was calculated with CYLTRANP. As the lead shielding is increased, the dose drops, but its uncertainty in the CYLTRANP prediction increases. However, if one chooses two larger detectors with vertical spans from 10 to 50 cm and 50 to 90 cm, respectively, as shown in figure 7, the dose variation over such detectors is fairly mild and the uncertainty will drop. This circumstance is the justification for the use of Detectors 1 and 2.

To reduce the uncertainty, especially for the thickest lead shielding, very large histories were computed—as many as 60 million. The computations were supported in part by a grant of computer time from the Department of Defense High Performance Computing Modernization Program at the U.S. Army Research Laboratory (ARL) Major Shared Resource Center (MSRC). Silicon Graphics computers of the MSRC were used to compute these long histories. Sample CYLTRAN input is given in appendix A.

Figure 9. Spatial variation of dose rate or equivalent dose rate equivalent computed for detectors at a distance of 30 cm from reltron. (Detector positions are shown in figure 8 and the detector vertical positions are the same as those given by the ruler in figure 8. The uncertainty,  $\sigma$ , in the dose comes from the Monte Carlo calculation and is the standard deviation in the energy deposited into the water detectors from millions of computed histories.)



Beam current: 600 A peak with 2  $\mu$ s pulse @ 300 Hz and duty cycle of 1.5 min on, 15 min off

---

## 4. Results and Conclusions

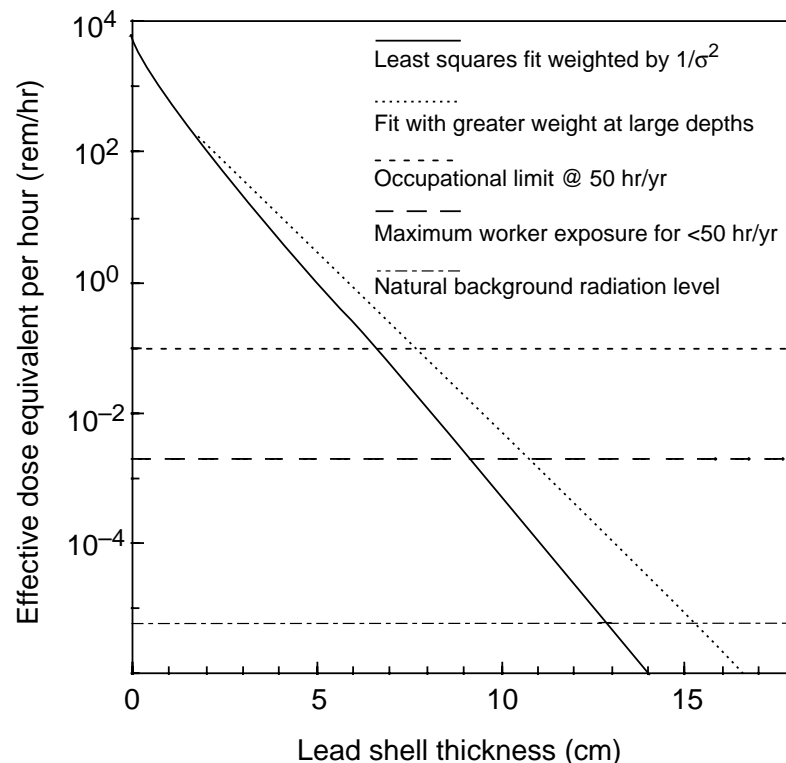
---

Figures 9 and 10 show results of the CYLTRANP calculations. In figure 10, the dose rate for Detector 1 is plotted as a function of the lead shielding thickness. Because the reltron would be elevated during actual use, the dose at locations with roughly the same elevation as the reltron measured by Detector 1 is more important than the dose above the reltron as measured by Detector 2.

Two fits made to the data of Detector 1 are shown in figure 10. One is least squares and is weighted with the reciprocal of the square of the uncertainty in the data. The other fit is less rigorous but gives more weight to the data at greater shielding thickness since the slope there should be [3] closer to the slope at greater thicknesses. Extrapolation of the latter fit to safe radiation levels gives a greater and therefore more conservative prediction of the required shielding thickness than does the rigorous fit.

The occupational radiological limit is 5 rem per year or 1.25 rem per quarter year, as established by the Occupational Safety and Health Administration [4]. This standard is only for special radiological workers or soldiers in battle and in practice, the radiological exposure is usually held to within 1/10th of these values. However, dividing the exposure into working hours, the occupational radiological limit becomes 0.1 rem/hr but is limited to exposures of 50 hr/yr. Because of the restrictions on the kinds of workers, this

Figure 10.  
Extrapolated fits of  
calculated dose rates  
or effective dose rate  
equivalent compared  
with safety standards.  
(The occupational  
limit given here is  
from the OSHA  
standard [4] divided  
into hours of  
exposure. The  
maximum worker  
exposure shown here  
is from Army  
regulation 11-9 [5].)



standard is not practical for a device that would be greatly used during less severe conditions. The standard maximum worker exposure is limited to 100 mrem/yr or 2 mrem/hr by Army regulation [5]. (This limit also applies to members of the general public.) Therefore, the dose rate of 0.002 rem/hr, which represents the standard maximum worker exposure level at 50 hr/yr, is the proper level at which to provide shielding.

The conservative extrapolation predicts that a shielding of 11 cm of lead provides protection better than this standard maximum worker exposure level if the exposure is no more than about 50 hr/year. It predicts that possibly as many as 100 hours of exposure per year at a level of 0.001 rad/hr could be achieved and still be within the standard maximum worker exposure level. Of course, this is just a prediction, and the dose produced by the reltron with these 11 cm of lead shielding in place would need to be measured to ascertain how many hours of exposure per year could be permitted.

The weight of 11 cm of lead shielding just for the compact anode section alone would be 878 lb. Because of a significant amount of X-ray scattering downward, the lower part of the reltron would also have to be shielded. The far greater bulk of the lower part of the reltron would require an even larger mass of lead shielding. The mass attenuation of the radiation through lead is much greater than the geometrical reduction factor at the shield radii. Therefore, the weight of this extra required shielding would scale roughly as the square of the radii of the lower sections. Actual reltron section radii corresponding to the sections in figure 1 clearly suggest that the total shielding would weigh 1 to 2 tons or more.

The X-ray calculations were meant to be a worst case result, since protection of the reltron users is the concern here. However, further calculations with more refined models could probably reduce the predicted X-ray levels and therefore the required shielding. Specifically, refining the model of how the beam strikes the anode would considerably reduce the levels of predicted lateral X-ray fluence. Also, the use of different shielding materials might reduce shielding requirements but probably only slightly.

---

## References

---

1. Goplen, B., L. Ludekind, D. Smithe, and G. Warren, "MAGIC User's Manual," MRC/WDC-R-326, Mission Research Corporation, January, 1994.
2. Halbleib, J. A. , R. P. Kensek, T. A. Mehlhorn, G. D. Valdez, S. M. Seltzer, and M. J. Berger, "ITS Version 3.0: The Integrated TIGER Series of Coupled Electron/Photon Monte Carlo Transport Codes," SAND91 - 1634 • UC - 405, Sandia National Laboratories, March 1992.
3. Radiological Health Handbook, January, 1970, U.S. Department of Health, Education, and Welfare, Public Health Service.
4. OSHA 29 CFR 1910.1096, Radiation Safety Manual, U.S. Department of Health and Human Services, Public Health Service, Centers for Disease Control and Prevention, Atlanta, GA, August 1999.
5. AR 11-9 May 28, 1999 Table 5-1 gives 100 mrem/yr as the maximum worker exposure. Paragraph 5-2, Footnote 4 gives 2 mrem as the maximum worker exposure in 1 hour.



---

## Appendix A. Sample CYLTRAN Input File

---

### Sample CYLTRAN Input

ECHO 1

TITLE

...1.14 MEV MAX, 2 CM PB TEST PROBLEM

\*\*\*\*\* GEOMETRY \*\*\*\*\*

\* ZMIN ZMAX RMIN RMAX MATERIAL NPHI NRHO NZ CUTOFF FORCING

GEOMETRY 36

0.0	11.63	0.0	4.76	0	1	1	1
0.0	11.63	4.76	5.99	1	1	1	1
0.0	18.51	5.99	6.14	0	1	1	1
0.0	22.43	6.14	6.47	1	1	1	1
11.63	12.63	0.0	4.51	0	1	1	1
11.63	12.63	4.51	5.99	1	1	1	1
12.63	13.63	0.0	4.01	0	1	1	1
12.63	13.63	4.01	5.99	1	1	1	1
13.63	14.63	0.0	3.51	0	1	1	1
13.63	14.63	3.51	5.99	1	1	1	1
14.63	15.63	0.0	3.01	0	1	1	1
14.63	15.63	3.01	5.99	1	1	1	1
15.63	16.63	0.0	2.51	0	1	1	1
15.63	16.63	2.51	5.99	1	1	1	1
16.63	17.63	0.0	2.01	0	1	1	1
16.63	17.63	2.01	5.99	1	1	1	1
17.63	18.51	0.0	1.51	0	1	1	1
17.63	18.51	1.51	5.99	1	1	1	1
18.51	20.26	0.0	1.27	0	1	1	1
18.51	19.51	1.27	4.99	1	1	1	1
18.51	19.51	4.99	6.14	0	1	1	1
19.51	20.26	1.27	3.99	1	1	1	1
19.51	20.51	3.99	6.14	0	1	1	1
20.26	20.51	0.0	3.99	1	1	1	1
20.51	21.51	0.0	2.99	1	1	1	1
20.51	21.51	2.99	6.14	0	1	1	1
21.51	22.43	0.0	2.53	1	1	1	1
21.51	22.43	2.53	6.14	0	1	1	1
22.43	30.0	0.0	6.32	2	1	1	1
22.43	30.0	6.32	6.47	0	1	1	1
0.0	30.0	6.47	8.47	4	1	1	1

30.0	32.0	0.0	8.47	4	1	1	1
32.0	90.0	0.0	8.47	0	1	1	1
0.0	90.0	8.47	30.0	0	1	1	1
0.0	10.0	30.0	37.0	0	1	1	1
10.0	90.0	30.0	37.0	2	1	1	2

\*\*\*\*\* SOURCE \*\*\*\*\*

ELECTRONS

SPECTRUM 45

1.00	0.99	0.98	0.97	0.95	0.94	0.93	0.921	.92	0.911	0.91	0.891	0.89
0.881	0.88	0.879	0.86	0.85	0.849	0.84	0.839	0.83	0.821	0.82	0.81	0.80
0.79	0.78	0.779	0.761	0.76	0.75	0.73	0.70	0.69	0.66	0.53	0.42	0.32
0.29	0.21	0.12	0.06	0.03	0.00							
1.14	1.12	1.09	1.07	1.04	1.01	0.99	0.96	0.94	0.91	0.88	0.86	0.83
0.81	0.78	0.75	0.73	0.70	0.68	0.65	0.62	0.60	0.57	0.55	0.52	0.49
0.47	0.44	0.42	0.39	0.36	0.34	0.31	0.29	0.26	0.23	0.21	0.18	0.16
0.13	0.10	0.08	0.05	0.03	0.00							

CUTOFFS 0.01 0.001

POSITION 0.0 0.0 0.0

RADIUS 0.0

\* DEFAULT DIRECTION

DIRECTION 0.0 0.0

\*\*\*\*\* OUTPUT OPTIONS \*\*\*\*\*

PHOTON-ESCAPE

NBINE 9

NBINT 18

PHOTON-FLUX 36 36

NBINE 9

NBINT 18

\*\*\*\*\* OTHER OPTIONS \*\*\*\*\*

HISTORIES 60000000

BATCHES 40

\* ... X-RAY PRODUCTION SCALING

SCALE-BREMS 500.

RANDOM-NUMBER

1014399783

## Distribution

Admnstr  
Defns Techl Info Ctr  
ATTN DTIC-OCF  
8725 John J Kingman Rd Ste 0944  
FT Belvoir VA 22060-6218

DARPA  
ATTN S Welby  
3701 N Fairfax Dr  
Arlington VA 22203-1714

Defns Threat Reduction Agcy  
ATTN DTRA/ESE D Devany  
6801 Telegraph Rd  
Alexandria VA 22310-3398

Ofc of the Secy of Defns  
ATTN ODDRE (R&AT)  
The Pentagon  
Washington DC 20301-3080

AMCOM MRDEC  
ATTN AMSMI-RD W C McCorkle  
Redstone Arsenal AL 35898-5240

US Army TRADOC  
Battle Lab Integration & Techl Dirctr  
ATTN ATCD-B  
FT Monroe VA 23651-5850

US Military Acdmy  
Mathematical Sci Ctr of Excellence  
ATTN MADN-MATH MAJ M Huber  
Thayer Hall  
West Point NY 10996-1786

Dir for MANPRINT  
Ofc of the Deputy Chief of Staff for Prsnl  
ATTN J Hiller  
The Pentagon Rm 2C733  
Washington DC 20301-0300

SMC/CZA  
2435 Vela Way Ste 1613  
El Segundo CA 90245-5500

TACOM Rsrch Dev & Engrg Ctr  
ATTN G Kahlil  
ATTN T Burke  
PO Box 249  
Warren MI 48090-0249

TECOM  
ATTN AMSTE-CL  
Aberdeen Proving Ground MD 21005-5057

US Army ARDEC  
ATTN AMSTA-AR-TD  
Bldg 1  
Picatinny Arsenal NJ 07806-5000

US Army Belvoir RDEC  
ATTN SATBE-FGE J Ferrick  
FT Belvoir VA 22060

US Army CECOM RDEC  
ATTN AMSEL-RD-NV-OD R Irwin  
FT Monmouth NJ 07703-5206

US Army CECOM RDEC NVESD  
ATTN AMSEL-RD-NV-CD-MN W D Lee  
10221 Burback Rd Ste 430  
FT Belvoir VA 22060-5806

US Army Commctn-Electronics Cmnd  
NVESD  
ATTN AMSEL-RD-NV-CD-MN S Schaedel  
10221 Burbeck Rd Ste 430  
FT Belvoir VA 22060-5806

US Army Info Sys Engrg Cmnd  
ATTN AMSEL-IE-TD F Jenia  
FT Huachuca AZ 85613-5300

US Army Intlgn & Info Warfare Dirctr  
ATTN AMSEL-RD-IW D Helm  
Bldg 600  
FT Monmouth NJ 07703-5211

US Army Natick RDEC Acting Techl Dir  
ATTN SBCN-T P Brandler  
Natick MA 01760-5002

## Distribution (cont'd)

US Army Simulation Train & Instrmntn  
Cmnd  
ATTN AMSTI-CG M Macedonia  
ATTN J Stahl  
12350 Research Parkway  
Orlando FL 32826-3726

US Army Tank-Automtv & Armaments Cmnd  
ATTN AMSTA-TR-R-MS-263 D Templeton  
Warren MI 48397-5000

US Army Tank-Automtv Cmnd RDEC  
ATTN AMSTA-TR J Chapin  
Warren MI 48397-5000

Cmnd Ofcr Nav Rsrch Lab  
ATTN Code 6843 D Abe  
4555 Overlook Ave SW  
Washington DC 20375-5320

Nav Rsrch Lab  
ATTN Code 5740 P C Grounds  
ATTN Code 6650 T Wieting  
4555 Overlook Ave SW  
Washington DC 20375-5000

Nav Surf Warfare Ctr  
ATTN Code B07 J Pennella  
17320 Dahlgren Rd Bldg 1470 Rm 1101  
Dahlgren VA 22448-5100

Air Force Rsrch Lab (Phillips Ctr)  
ATTN AFRL W L Baker Bldg 413  
3550 Aberdeen Ave SE  
Kirtland NM 87112-5776

US Air Force Phillips Lab  
ATTN K Hackett  
3550 Aberdeen Ave SE  
Kirtland Air Force Base NM 87117-5776

Hicks & Assoc Inc  
ATTN G Singley III  
1710 Goodrich Dr Ste 1300  
McLean VA 22102

Mission Rsrch Corp  
ATTN M Bollen  
ATTN R Smith  
8560 Cinderbed Rd Ste 700  
Newington VA 22122

Mission Rsrch Corp  
ATTN J Havey  
ATTN S Graybill  
1720 Randolph Rd SE  
Albuquerque NM 87106-4245

NorthStar Rsrch  
ATTN R Richter-Sand  
4421 A McLeod NE  
Albuquerque NM 87109

Palisades Inst for Rsrch Svc Inc  
ATTN E Carr  
1745 Jefferson Davis Hwy Ste 500  
Arlington VA 22202-3402

Director  
US Army Rsrch Lab  
ATTN AMSRL-RO-D JCI Chang  
ATTN AMSRL-RO-EN W D Bach  
PO Box 12211  
Research Triangle Park NC 27709

US Army Rsrch Lab  
ATTN AMSRL-CI-IS-R Mail & Records Mgmt  
ATTN AMSRL-CI-IS-T Techl Pub (2 copies)  
ATTN AMSRL-CI-OK-TL Techl Lib (2 copies)  
ATTN AMSRL-CS-RK-S M Borisky  
ATTN AMSRL-D D R Smith  
ATTN AMSRL-DD J M Miller  
ATTN AMSRL-SE-D E Scannell  
ATTN AMSRL-SE-DE C Kenyon (12 copies)  
ATTN AMSRL-SE-DP A Bromborsky  
ATTN AMSRL-SE-DP C Lazard  
ATTN AMSRL-SE-DP K Kerris  
ATTN AMSRL-SE-DP M Litz  
ATTN AMSRL-SE-DP R A Kehs  
ATTN AMSRL-SE-DS G Merkel  
ATTN AMSRL-SE-DS M Berry  
ATTN AMSRL-SE-DS W O Coburn  
Adelphi MD 20783-1197

<b>REPORT DOCUMENTATION PAGE</b>			<i>Form Approved OMB No. 0704-0188</i>	
<small>Public reporting burden for this collection of information is estimated to average 1 hour per response, including the time for reviewing instructions, searching existing data sources, gathering and maintaining the data needed, and completing and reviewing the collection of information. Send comments regarding this burden estimate or any other aspect of this collection of information, including suggestions for reducing this burden, to Washington Headquarters Services, Directorate for Information Operations and Reports, 1215 Jefferson Davis Highway, Suite 1204, Arlington, VA 22202-4302, and to the Office of Management and Budget, Paperwork Reduction Project (0704-0188), Washington, DC 20503.</small>				
<b>1. AGENCY USE ONLY</b> <i>(Leave blank)</i>		<b>2. REPORT DATE</b> October 2001	<b>3. REPORT TYPE AND DATES COVERED</b> Final, 6/99 to 12/00	
<b>4. TITLE AND SUBTITLE</b> X-ray Shielding Requirements for a Reltron			<b>5. FUNDING NUMBERS</b> DA PR: AH94 PE: 62705A	
<b>6. AUTHOR(S)</b> Christopher S. Kenyon				
<b>7. PERFORMING ORGANIZATION NAME(S) AND ADDRESS(ES)</b> U.S. Army Research Laboratory Attn: AMSRL-SE-DP email: ckenyon@arl.army.mil 2800 Powder Mill Road Adelphi, MD 20783-1197			<b>8. PERFORMING ORGANIZATION REPORT NUMBER</b> ARL-TR-2440	
<b>9. SPONSORING/MONITORING AGENCY NAME(S) AND ADDRESS(ES)</b> U.S. Army Research Laboratory 2800 Powder Mill Road Adelphi, MD 20783-1197			<b>10. SPONSORING/MONITORING AGENCY REPORT NUMBER</b>	
<b>11. SUPPLEMENTARY NOTES</b> ARL PR: 1NE6XX AMS code: 622705.H94				
<b>12a. DISTRIBUTION/AVAILABILITY STATEMENT</b> Approved for public release; distribution unlimited.			<b>12b. DISTRIBUTION CODE</b>	
<b>13. ABSTRACT</b> <i>(Maximum 200 words)</i> Radiological dose rates from X-rays produced by a reltron (relativistic electron tube) microwave tube are calculated via standard electron-photon Monte Carlo transport software from the Integrated TIGER* Series developed by Sandia National Laboratories, Albuquerque, NM. Comparison of an extrapolation of this dose rate for several hypothetical thicknesses of lead shielding surrounding this reltron with the standard maximum worker-allowed radiation level predicts the thickness of lead shielding required in the design of the reltron. Using worst case modeling for the X-rays, the required amount of lead shielding is, roughly, 1 ton.  *TIGER is not an acronym				
<b>14. SUBJECT TERMS</b> High power microwaves, reltron, X-ray, radiation shielding			<b>15. NUMBER OF PAGES</b> 24	
			<b>16. PRICE CODE</b>	
<b>17. SECURITY CLASSIFICATION OF REPORT</b> Unclassified	<b>18. SECURITY CLASSIFICATION OF THIS PAGE</b> Unclassified	<b>19. SECURITY CLASSIFICATION OF ABSTRACT</b> Unclassified	<b>20. LIMITATION OF ABSTRACT</b> UL	